



Prominence Formation and Oscillations

P. F. Chen^{1,2*}

¹*Department of Astronomy, Nanjing University, Nanjing 210093, China*

²*Key Lab of Modern Astron. & Astrophys. (Ministry of Education), Nanjing University, China*

Received 26th June 2018

Abstract. Prominences, or filaments, are a striking phenomenon in the solar atmosphere. Besides their own rich features and dynamics, they are related to many other activities, such as solar flares and coronal mass ejections (CMEs). In the past several years we have been investigating the prominence formation, oscillations, and eruptions through both data analysis and radiative hydrodynamic and magnetohydrodynamic (MHD) simulations. This paper reviews our progress on these topics, which includes: (1) With updated radiative cooling function, the coronal condensation becomes a little faster than previous work; (2) Once a seed condensation is formed, it can grow via siphon flow spontaneously even if the evaporation stops; (3) A scaling law was obtained to relate the length of the prominence thread to various parameters, indicating that higher prominences tend to have shorter threads, which is consistent with the fact that threads are long in active region prominences and short in quiescent prominences; (4) It was proposed that long-time prominence oscillations out of phase might serve as a precursor for prominence eruptions and CMEs; (5) An ensemble of oscillating prominence threads may explain the counter-streaming motion.

Keywords : Sun: filaments – Sun: prominences – Sun: coronal mass ejections (CMEs)

1. Introduction

Filaments are striking features in the solar atmosphere, typically observed in chromospheric lines like $H\alpha$. They are also identifiable in EUV images. Against the solar disk, they appear as long filamentary structures, by which the phenomenon was

*email: chenpf@nju.edu.cn

called. When they appear above the solar limb, it was recognized that they are dense plasma suspended in the hot tenuous corona. In this case they are called prominences. The two terminologies are used interchangeably in the literature. With the temperature ~ 100 times lower and the density ~ 100 times higher than the ambient corona, prominences are interesting to researchers in various aspects. Their formation and dynamics are related to the energy transport (heating and cooling) and force balance (Low et al. 2012) in the corona; Their oscillations can be applied to diagnose the magnetic field where the prominence is embedded; Their eruptions are then directly related to solar flares and coronal mass ejections (CMEs). It has been established that the erupting prominence is the core of the CME (House et al. 1981). Here we emphasize that prominences might also be the core of CME researches. This is reflected in the various aspects of the CME-related researches. First, prominences are formed in highly sheared magnetic field, including flux ropes and sheared arcades, where the long flux tubes favor thermal instability by which prominences are often believed to be formed. Highly sheared magnetic field is also a signature of the non-potentiality of the magnetic system which possesses sufficient magnetic free energy to power CMEs. Second, the initiation of the filament might well correspond to the onset of CMEs, when the CME frontal loop has not yet formed (Chen 2011). In particular, the mass drainage from the prominence might serve as one possible triggering mechanism for CMEs. Third, prominences are the core of the CMEs and the magnetic cloud of interplanetary CMEs. Fourth, regarding the debate whether the flux rope is formed before or during CME eruptions (Zhang, Cheng & Ding 2012; Cheng et al. 2013), Chen (2011) suggested that in many cases a flux rope exists in the progenitor of the CME, which corresponds to the eruption of an inverse-polarity prominence, whereas in other cases the flux rope is formed during CME eruption via magnetic reconnection, which corresponds to the eruption of a normal-polarity prominence.

There are several detailed review papers on prominences (Martin 1998; Labrosse et al. 2010; Mackay et al. 2010; Schmieder & Aulanier 2012). In this paper, we summarize what my group have done on prominences in recent years, with the purpose to clarify what are the best follow-up researches in the foreseeable future. The topics cover the formation, dynamics, oscillations, and eruptions of prominences.

2. Formation mechanism

The formation mechanisms of cold prominence plasma remain to be a controversial issue. As reviewed by Mackay et al. (2010), there are basically two mechanisms, i.e., direct injection model (from the chromosphere to the corona) and the evaporation-condensation model. The latter came from the idea of thermal instability of the coronal plasma (Parker 1953). Noticing that the coronal plasma along the flux tube is not sufficient to supply the necessary mass for the prominence thread, it has been proposed that there is chromospheric evaporation to the corona before condensation, which is driven by extra heating localized in the chromosphere (e.g., Poland & Mariska 1986). Such an evaporation-condensation model was numerically simulated by Mok et al. (1990), Antiochos et al. (1999), and Karpen & Antiochos

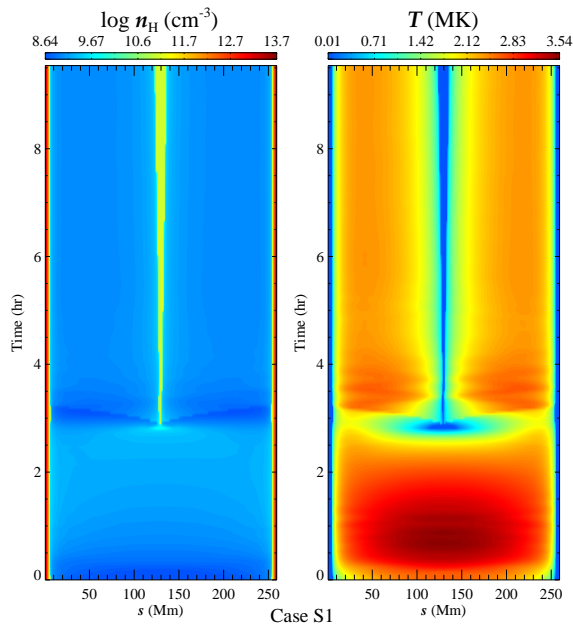


Figure 1. Temporal evolution of the plasma density (left) and the temperature (right) along the model loop in the case of symmetric heating. The two loop footpoints are at $s = 0$ and 260 Mm, respectively (from Xia et al. 2011).

(2008, and references therein), and was demonstrated to be able to explain various observational features. Note that all these simulations were done in one dimension (1D). This is validated since high-resolution observations indicate that prominences are composed of many narrow threads which are supposed to run along the individual magnetic flux tubes (Lin et al. 2008), and threads are the building blocks for prominences.

Following this line of thought, we adopted the recently updated radiative cooling function to numerically simulate the response of the solar atmosphere to the enhanced chromospheric heating by solving 1D radiative hydrodynamic equations (Xia et al. 2011). Figure 1 depicts the evolution of the density and temperature distributions along the magnetic loop in the case of symmetric heating. It is seen that with the heating rate $E_1 = 10^{-2} \text{ erg cm}^{-3} \text{ s}^{-1}$ in the chromosphere, the coronal condensation occurs 2.8 hr after the extra heating is introduced to the chromosphere. In contrast, the radiative cooling function used in Karpen et al. (2005) was 1-2 times lower than ours, and the coronal condensation occurs at $t = 3.5$ hr.

The evaporation-condensation model was recently directly confirmed by Liu et al. (2012) and Berger et al. (2012) with the EUV observations from *Solar Dynamics Observatory* (SDO), which showed that the enhanced emissions appeared in turn from

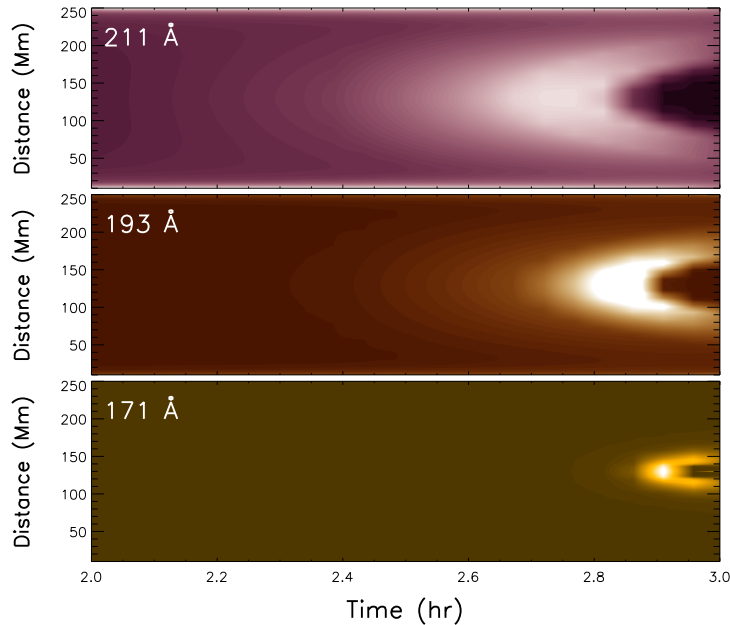


Figure 2. Temporal evolutions of EUV intensity distributions along the model loop at three wave bands, Fe XIV 211 Å, Fe XII 193 Å, and Fe IX 171 Å. The EUV intensity is calculated from the temperature and density distributions in Fig. 1.

higher-temperature wave band (211 Å) to lower-temperature wave band (171 Å) and all the way to He I 304 Å which is mainly from the cool prominence plasma. In order to compare our simulation results with the observations, we calculate the EUV intensity distribution along the magnetic loop, whose temporal evolutions at three wave bands are presented in Fig. 2. The numerical results are seen to be qualitatively consistent with observations very well, i.e., just before the prominence formation the strong EUV emission appears in the hot line (Fe XIV 211 Å) first, and then shifts to the lower-temperature lines successively. However, one big difference between our Fig. 2 and the Figure 3 of Berger et al. (2012) is that the time delay of the strong emissions between 171 Å and 211 Å is ~ 12 hr in Berger et al. (2012), whereas it is 12 min in our Fig. 2, i.e., 60 times shorter than in the observations. If the radiative cooling function is precise, there are two other possible reasons for the discrepancy. One is that the background heating rate might be under-estimated. The other is that the plasma density just prior to the coronal condensation in Berger et al. (2012) is many times smaller than the value in our simulations, i.e., $n = 2 \times 10^9 \text{ cm}^{-3}$, considering the radiative cooling timescale is proportional to $1/n$. In this case, if we want to explain the observations in Berger et al. (2012), the extra chromospheric heating rate used for Fig. 1, i.e., $E_1 = 10^{-2} \text{ erg cm}^{-3} \text{ s}^{-1}$, might be too large so that the strong evaporating flow compresses the coronal plasma at the loop apex to a high value. This issue should be investigated in the future. As far as Xia et al. (2011) can tell, the decreasing

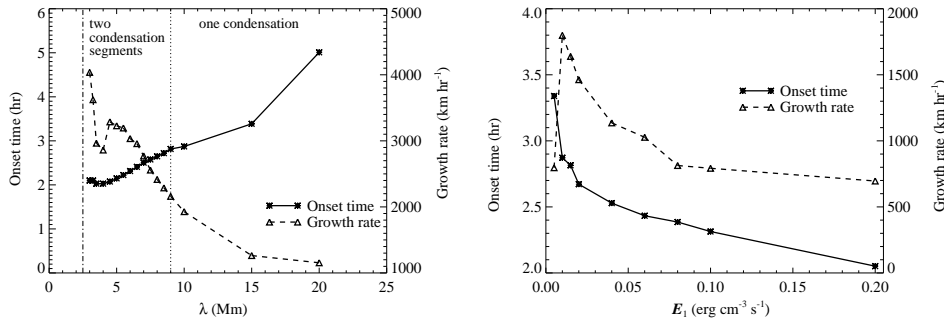


Figure 3. The dependence of the condensation onset time (asterisks) and the growth rate (triangles) on the amplitude (E_1) and the scale height (λ) of the extra chromospheric heating (from Xia et al. 2011).

E_1 does postpone the formation of prominences, and also increases the delay of EUV emissions from hot to warm wave bands.

3. Length and growth rate

Observations indicate that the threads of active region prominences are often long and the threads of quiescent prominences are short (Mackay et al. 2010). This is an interesting property which deserves a sound explanation. Apparently it may be directly related to the difference of the magnetic environment between the two types of prominences since active region prominences are generally low and quiescent prominences are located several times higher. Recently, we did a parameter survey on how the magnetic configuration influences the features of the prominences (Zhang et al. 2013). It is revealed that if other factors, e.g., the width and the depth of the magnetic dip, and the evaporation time, are kept the same, the length of the prominence thread (l) scales with the altitude (h) by $l \sim h^{-0.37}$, which implies that higher prominences tend to have shorter threads, which is consistent with observations.

The long thread is not formed at once. It grows from seed condensation in the corona. Various parameters may affect the growth rate of the prominence thread. Xia et al. (2011) found that both the amplitude (E_1) and the scale height (λ) of the extra chromospheric heating change the growth rate in a non-monotonic way. As shown by the triangles in Fig. 3, both weak and strong E_1 do not favor the fast growth of the prominence thread, whereas the growth rate decreases with increasing λ except a significant drop near $\lambda = 3.5$ Mm.

Xia et al. (2011) noted that once radiative instability happens near the loop apex due to chromospheric evaporation, the tradeoff of the decreasing temperature and the increasing density turns out that the gas pressure decreases to a value smaller than in the pre-evaporation stage. As a result, even if the extra chromospheric heating is

switched off, a siphon flow is formed naturally due to the loss of force balance which enables the initial static coronal loop: chromospheric plasma is siphoned up and then heated in the corona via background heating. When the siphon flow penetrates into the cold condensation near the loop apex, it is cooled via enhanced radiation. This implies that extra chromospheric heating is not necessary to maintain or grow the prominence thread. Once a seed condensation is formed, it would grow without the help of extra chromospheric heating and evaporation, although the growth rate is smaller than in the case with extra chromospheric heating. This property might be meaningful since the extra heating, which is responsible for the chromospheric evaporation, might be due to low-atmospheric magnetic reconnection (e.g., Chen, Fang & Ding 2001), which generally has a limited lifetime. It might be not realistic to have continual heating.

A further question arises following the above-mentioned simulations, that is, given a dipped magnetic loop, what is the maximum length that the prominence thread can grow. This question is being tackled currently (Zhou et al. 2014).

4. Oscillations

The solar corona is always dynamic, and disturbances are ubiquitous, e.g., from sporadic CMEs, flares or subflares, to the non-stopping convection flows in the photosphere, which drive kink/Alfvén waves into the corona (Tian et al. 2012). Therefore, once a prominence is formed it is subjected to all these disturbances, and is ready to oscillate. Prominence oscillations can be divided into large-amplitude versus small-amplitude ones, or transverse versus longitudinal ones (Arregui et al. 2012). The observational characteristics, including the period and damping timescale, can be used to diagnose the thermal and magnetic parameters of the prominences. Since longitudinal oscillations can be simulated in 1D, we investigated this topic as a start for its simplicity.

With the magnetic geometry derived from observations, we (Zhang et al. 2012) numerically simulated the prominence oscillations, as depicted in Fig. 4, which shows the temporal evolutions of the density and the temperature distributions along the magnetic loop. We found that the simulations can reproduce the period of the longitudinal prominence oscillation which was observed on 2007 February 8, though the resulting damping timescale is 1.5 times longer than the observational value.

Recently, we (Zhang et al. 2013) did a parameter survey about the characteristics of prominence oscillations. We first compared the effect of the trigger type, i.e., localized heating or impulsive momentum from a nearby subflare., which turned out to be that the oscillation is nearly independent of the trigger type. It was found that with the presence of non-adiabatic terms including thermal conduction and radiative cooling the oscillation would damp out, where the radiative cooling was demonstrated to be dominant. Scaling laws were obtained to relate the oscillation period (P) and decay timescale (τ) to various parameters, i.e., $P \sim 2\pi \sqrt{R/g_\odot}$, where R is the curvature radius of the magnetic dip, and $\tau \sim l^{1.63} D^{0.66} w^{-1.21} v_0^{-0.30}$, where l is the prominence

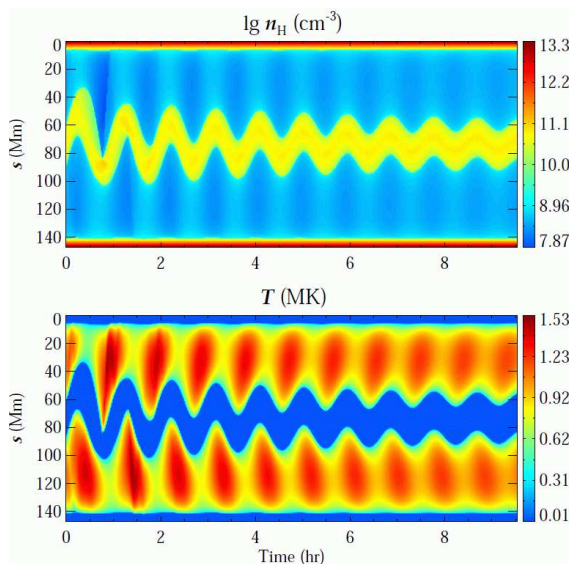


Figure 4. Time evolutions of the density (*top*) and the temperature (*bottom*) distributions along the magnetic loop, which indicate that the prominence experiences a damped oscillation subjected to a perturbation (from Zhang et al. 2012).

length, D and w are the depth and the width of the magnetic dip, and v_0 the velocity perturbation amplitude. The scaling law for P , which is the same for a pendulum, implies that the field-aligned component of the gravity is the main restoring force for the longitudinal oscillations, as also found by Luna & Karpen (2012).

Besides the scaling laws, two more results are worth mentioning. One is that we found that if a subflare occurs immediately near the footpoints of the magnetic loops running through the prominence, $\sim 4\%$ of the released thermal energy would be converted to the kinetic energy of the prominence oscillation. The other one is that we found that mass drainage from the prominence to the chromosphere would significantly damp the oscillation.

5. Long-time oscillation as a precursor for CMEs

Generally prominence oscillations damp in ~ 3 – 4 periods, as found both in observations and simulations mentioned above. However, sometimes the prominence oscillation may persist for much longer time. With SUMER spectrometer, we presented a case where a prominence oscillated for 12 periods before eruption (Chen, Innes & Solanki 2008), as displayed in Fig. 5. With that, we proposed that long-time prominence oscillation may be a precursor for prominence eruptions and CMEs.

Such a proposal was backed by recent two examples, and in both events the prom-

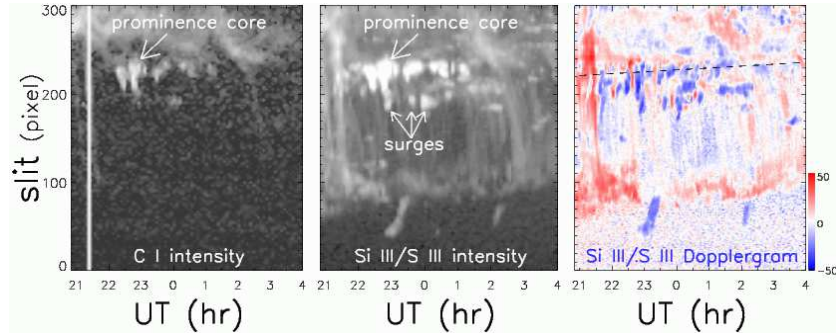


Figure 5. Left panel: Evolution of the C I 1118.45 Å intensity along the SUMER slit; Middle panel: Same for S III/Si III 1113 Å; Right panel: Evolution of the Dopplergram along the the SUMER slit observed at S III/Si III 1113 Å (from Chen, Innes & Solanki 2008).

inence was oscillating longitudinally before eruption. With *Hinode* and *SOHO* observations, Zhang et al. (2012) analyzed an event where only a thread of a prominence erupted to form a CME, with the main body remaining at the original height. They found that before the thread eruption, the whole prominence body was oscillating along its spine. With high-resolution observations from *SDO*, Li & Zhang (2012) revealed the longitudinal oscillation and the ensuing eruption of the whole filament, where plasma drainage from the oscillating filament to the solar surface may facilitate the onset of the eruption.

Such prominence oscillations would continue in the later eruption phase as revealed by Isobe & Tripathi (2006) and Mierla et al. (2012).

6. Counter-streaming

Counter-streaming of plasma was found in prominences (Zirker et al. 1998). Its nature is still unclear, and we are still not sure whether it is common in any prominence at any time or it is a signature of prominence activation.

The first possibility is favored by the longitudinal prominence oscillations. The longitudinal oscillations can be extrinsic, i.e., being triggered by a nearby subflare, or intrinsic, i.e., through asymmetric heating at the two footpoints of the magnetic loop. Similar to Antiochos et al. (1999) and Luna & Karpen (2012), we (Xia et al. 2011) found that if the extra chromospheric heating is asymmetric at the two footpoints of the magnetic loop, the prominence, upon formation, would oscillate around the magnetic dip or even flow along the loop to drain down toward the footpoint with weaker heating and then repeat the formation-drainage cycle, as illustrated by Fig. 6. The prominence thread experiences oscillations while moving to the right. Counter-streaming might just be an ensemble of oscillating threads which are not in phase (a similar idea was mentioned by Ahn et al. 2010). In practice, even if the oscillations

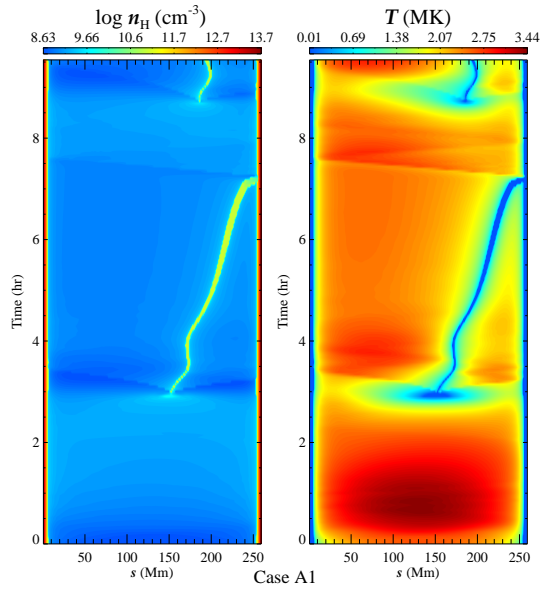


Figure 6. Temporal evolution of the plasma density (*left*) and the temperature (*right*) along the model loop in the asymmetric. The loop footpoints are at $s = 0$ and 260 Mm, respectively (from Xia et al. 2011).

of different threads are in phase initially, they would evolve to be out of phase since different threads have different oscillation periods. Furthermore, even in the case without longitudinal oscillations, counter-streamings may still appear if the footpoint heating is randomly distributed in the solar surface, which drives mass drainage in a random way, i.e., the drainage is toward the positive magnetic polarity in some threads and toward the negative polarity in others. With these possibilities, we speculate that counter-streaming may not necessarily be the precursor for prominence eruptions and CMEs. However, the significant change of the counter-streaming might serve as a precursor for prominence eruptions and CMEs, which should be clarified in the future. Our recent results suggest that both longitudinal and interlaced uni-directional flows contribute to counter-streamings (Chen et al. 2014).

7. Prospects

Aided by the high-resolution multi-wavelength observations from various telescopes, more and more detailed features of prominences and their dynamics are being revealed, which provide evidence for the evaporation-condensation model and open new windows for theoretical (Low et al. 2012) and numerical studies (Xia et al. 2011; Luna & Karpen 2012). Such a model, which was numerically realized only in 1D radiative hydrodynamics until 2011, was extended to 2.5D MHD by Xia et al. (2012),

while its extension to 3D MHD is also on-going, which will be crucial to the understanding of the detailed observations of prominences.

Acknowledgements

PFC is grateful to the SOC members for the invitation to present the review paper and to my students for their contributions. This work was financially supported by Chinese foundations 2011CB811402 and NSFC (11025314, 10878002, and 10933003).

References

- Ahn, K., Chae, J., Cao, W., & Goode, P. R. 2010, *ApJ*, 721, 74
- Antiochos, S. K., MacNeice, P. J., Spicer, D. S., Klimchuk, J. A. 1999, *ApJ*, 512, 985
- Arregui, I., Oliver, R., & Ballester, J. L. 2012, *Living Reviews in Solar Physics*, 9, 2
- Berger, T. E., Liu, W., & Low, B. C. 2012, *ApJ*, 758, L37
- Chen, P. F., 2011, *Living Reviews in Solar Physics*, 8, 1
- Chen, P.-F., Fang, C., & Ding, M.-D. 2001, *Chinese J. Astron. Astrophys.*, 1, 176
- Chen, P. F., Harra, L. K., & Fang, C. 2014, *ApJ*, 784, 50
- Chen, P. F., Innes, D. E., & Solanki, S. K. 2008, *A&A*, 484, 487
- Cheng, X., Zhang, J., Ding, M. D., Liu, Y., & Poomvises, W. 2013, *ApJ*, 763, 43
- House, L. L., Wagner, W. J., Hildner, E. et al. 1981, *ApJ*, 244, L117
- Isobe, H., & Tripathi, D. 2006, *A&A*, 449, L17
- Karpen, J. T., Antiochos, S. K. 2008, *ApJ*, 676, 658
- Karpen, J. T., Tanner, S. E. M., Antiochos, S. K., DeVore, C. R. 2005, *ApJ*, 635, 1319
- Labrosse, N., Heinzel, P., Vial, J.-C., et al. 2010, *Space Sci. Rev.*, 151, 243
- Li, T., & Zhang, J. 2012, *ApJ*, 760, L10
- Lin, Y., Martin, S. F., & Engvold, O. 2008, *ASP Conference Series*, 383, 235
- Liu, W., Berger, T. E., & Low, B. C. 2012, *ApJ*, 745, L21
- Low, B. C., Berger, T., Casini, R., & Liu, W. 2012, *ApJ*, 755, 34
- Luna, M., & Karpen, J. 2012, *ApJ*, 750, L1
- Mackay, D. H., Karpen, J. T., Ballester, J. L., Schmieder, B., & Aulanier, G. 2010, *Space Sci. Rev.*, 151, 333
- Martin, S. F. 1998, *Solar Phys.*, 182, 107
- Mierla, M., Seaton, D. B., Berghmans, D., et al. 2012, *Solar Phys.*, 66
- Mok, Y., Drake, J. F., Schnack, D. D., & van Hoven, G. 1990, *ApJ*, 359, 228
- Parker, E. N. 1953, *ApJ*, 117, 431
- Poland, A. I., & Mariska, J. T. 1986, *Solar Phys.*, 104, 303
- Schmieder, B., & Aulanier, G. 2012, *EAS Publications Series*, 55, 149
- Tian, H., McIntosh, S. W., Wang, T., et al. 2012, *ApJ*, 759, 144
- Xia, C., Chen, P. F., Keppens, R., & van Marle, A. J. 2011, *ApJ*, 737, 27
- Xia, C., Chen, P. F., & Keppens, R. 2012, *ApJ*, 748, L26
- Zhang, J., Cheng, X., & Ding, M.-D. 2012, *Nature Communications*, 3, 747
- Zhang, Q. M., Chen, P. F., Xia, C., & Keppens, R. 2012, *A&A*, 542, A52
- Zhang, Q. M., Chen, P. F., Xia, et al., Keppens, R., & Ji, H. S. 2013, *A&A*, 554, A124

- Zhou, Y. H., Chen, P. F., Zhang, Q. M., & Fang, C. 2014, RAA, 14, 581
Zirker, J. B., Engvold, O., & Martin, S. F. 1998, Nature, 396, 440